European Journal of Medicinal Chemistry Reports 10 (2024) 100127

Contents lists available at ScienceDirect

European Journal of Medicinal Chemistry Reports

journal homepage: www.editorialmanager.com/ejmcr/default.aspx

Functionalized methoxy quinoline derivatives: Experimental and in silico evaluation as new antiepileptic, anti-Alzheimer, antibacterial and antifungal drug candidates

Bilge Çiftci[a], Salih Ökten[b,*], Ümit Muhammet Koçyiğit[c], Vildan Enisoğlu Atalay[d], Mehmet Ataş[c], Osman Çakmak[e]

[a] Vocational School of Health Services, Bilecik Şeyh Edebali University, Bilecik, Turkiye
[b] Department of Maths and Science Education, Faculty of Education, Kırıkkale University, Yahşihan, Kırıkkale, Turkiye
[c] Department of Basic Pharmaceutical Sciences, Faculty of Pharmacy, Sivas Cumhuriyet University, Sivas, Turkiye
[d] Department of Molecular Biology and Genetics, Faculty of Engineering and Natural Sciences, Üsküdar University, Üsküdar, İstanbul, Turkiye
[e] Department of Gastronomy, Faculty of Arts, Design and Architecture, İstanbul Rumeli University, Silivri, İstanbul, Turkiye

ARTICLE INFO

Keywords:
Acetylcholinesterase enzyme inhibition
Carbonic anhydrase enzyme inhibition
Methoxyquinoline
Quinoline

ABSTRACT

The objective of this study was to assess the inhibitory effects of newly synthesized quinoline derivatives on human carbonic anhydrase I and II (hCA I and II), as well as acetylcholinesterase (AChE) enzymes, alongside their impact on various microorganisms. The synthesized compounds were assessed using IC_{50}, K_i and MIC values via Ellman and Esterease Method and Microdilution assay. Most compounds exhibited strong inhibitory effects on human carbonic anhydrase I and II (hCA I and II) and acetylcholinesterase (AChE), notably compounds **9**, **12**, and **17** for hCA I, and **9**, **12**, **16** and **17** for hCA II, alongside robust AChE inhibition by compounds **8** and **13**. Antimicrobial tests highlighted compounds **13** and **15** as promising inhibitors against pathogens, particularly effective across various strains. Molecular docking supported these findings, indicating potent binding abilities, notably by compounds **16** and **17** across specific protein structures (2COP, 5E2M, and 6KM3). The discussion emphasized the impact of substituents, particularly methoxy groups at specific positions, on enzyme inhibition, revealing how structural modifications affected enzyme inhibitory properties. The comprehensive analysis bridged experimental and computational findings, uncovering essential structure-activity relationships in quinoline derivatives and identifying potential candidates for further studies in enzyme inhibition and antimicrobial research.

1. Introduction

Quinoline ring is an important biologically active heterocyclic ring with high applicability in pharmaceutical field and widely used [1]. The quinoline structure is similar to the pyridine and benzene rings, which are fused together with adjacent carbons [2].

Quinoline is a cyclic structure that occurs as a structural component in various natural and synthetic compounds, and its scaffold is derivatizable. This unique property of quinoline explains its broad range of biological activities [3–7] which makes it a privileged substance in the field of drug design. Over the last decade, the quinoline structure has been widely utilized for drug design, mainly due to its versatile properties, in order to investigate potential treatments for various diseases, such as antimalarials (chloroquine), antivirals (saquinavir), antibacterials (ciprofloxacin), antifungals, antiprotozoals (clioquinol), anti-asthmatic agents (montelukast), anticancer agents (irinotecan), anti-tumor, anti-covid and antipsychotics (aripiprazole) [8–14]. The effective antimicrobial activity of 6-methoxyquinoline derivatives against gram-positive and gram-negative bacteria, as well as their antifungal effects against certain fungal species, have been reported in recent literature [15]. A series of 8-amino-6-methoxyquinoline hybrids, synthesized through the Ugi-azide reaction, exhibited potent antiplasmodial activity and low [16]. Additionally, aryl-substituted 6-methoxyquinoline derivatives have been found to exhibit potential P-glycoprotein inhibition activity at low IC_{50} values [17].

In the process of developing new compounds, it is crucial to consider

* Corresponding author. Kırıkkale University, Faculty of Education, Department of Maths and Science Education, 71450, Yahşihan, Kırıkkale, Turkiye.
E-mail addresses: salihokten@kku.edu.tr, sokten@gmail.com (S. Ökten).

https://doi.org/10.1016/j.ejmcr.2023.100127
Received 16 October 2023; Received in revised form 12 December 2023; Accepted 13 December 2023
Available online 17 December 2023

their physicochemical properties, such as molecular weight, polar surface area, and the number of hydrogen bond donors and acceptors. These factors play a crucial role in determining whether the molecule can cross the blood-brain barrier (BBB) or not [18]. Failure to cross the BBB can result in the drug being metabolized before it can exert its therapeutic effect due to systemic enzymatic attack and opsonization of plasma proteins in the peripheral circulation [19].

In the development of drugs for neurodegenerative diseases such as Alzheimer's disease (AD) and epilepsy, it becomes even more important to ensure that the drug can cross the BBB. Quinoline derivatives have been studied in this regard, and it has been reported by Fiorito et al. that the quinoline derivative they synthesized was able to pass the BBB in their study [20].

Epilepsy is a neurological disorder that affects approximately 65 million people worldwide [21], characterized by abnormal and excessive neuronal firing in the brain, leading to seizures [22]. hCAs are enzymes that regulate extracellular and intracellular pH, and their inhibition is a potential method of treating epilepsy by increasing the level of CO_2 in the brain [23]. Although various antiepileptic drugs target hCAs, their lack of specificity leads to various side effects, and there is a need to develop more selective hCA inhibitors that can treat epilepsy more effectively and with fewer side effects [24,25]. The discovery of new sulfur-free drugs to inhibit hCA is gaining importance in this regard. In addition, there is a need for new antiepileptic drugs with fewer side effects and improved seizure control.

Alzhemier's Disease (AD) is the most common cause of dementia worldwide, characterized by cognitive and functional deficits, changes in patient behavior, problems with short-term memory, and poor visuospatial and executive functions [26]. Despite numerous studies on its pathophysiology, the exact cause of AD remains unclear. The most widely accepted hypotheses are the "amyloid hypothesis," which suggests that the accumulation of β-layers in the central nervous system causes dementia, and the "cholinergic hypothesis," which relates the loss of cholinergic function to memory impairments [27]. Treatment options based on these hypotheses aim to prevent the disease-causing factors. The discovery of new treatments and a better understanding of the pathophysiology of AD is necessary to improve the care of people with this disease [28].

Halogenated and nitrated aromatic heterocycles, such as quinoline and tacrine, have been found to possess increased biological activity in many cases and can also serve as useful intermediates for the synthesis of other molecules [29–31]. However, the structure-activity relationship analyses of previous studies have revealed that the presence of a methoxy substituent on the quinoline ring is crucial for achieving high therapeutic efficacy [32]. In our previous investigations, we examined the bioactivities of substituted quinolines against various cancer cells, metabolic enzymes, and bacterial strains. Our findings indicated that nitrated and brominated 6,8-dimethoxyquinoline analogues exhibit selective anticancer and antibacterial activity and effectively inhibit acetylcholinesterase (AChE), as well as cytosolic hCA isoenzymes [7,11]. Herein, we aimed to evaluate the anticholinergic and antiepileptic properties of methoxyquinoline and methoxyquinoline bromide derivatives based on their enzyme inhibitory potential. Our interest in this area was sparked by the significant enzyme inhibitory properties of quinoline derivatives reported in various studies.

2. Materials and methods

General. *p*-Nitrophenyl acetate, tris, acetylcholine iodate, 5,5′-Dithiobis (2-nitrobenzoic acid) (DTNB), carbonic anhydrase I - II isoenzymes and acetylcholinesterase purchased from Sigma-Aldrich.

Spectrophotometer (SOIFoptical Instruments/China) was used to measure the color intensity of the prepared mixture to determine enzyme activity. Magnetic stirrer (Electro- MAG/Turkey) was used to ensure that the prepared solutions were homogeneous. Precision balance (Weightlab Instrument/Turkey) was used to weigh the chemicals. pH meter (HANNA/United States) was used to measure the pH of the buffers. Vortex instrument (Velp Scientifica/Italy) was used to prepare homogeneous mixtures. Micropipette types (Weightlab/Turkey, Nichipet EXII/Japan, ISOLAB/Turkey, A.B.T. Laboratory Industry/Turkey) were used to transfer very small amounts of liquid (microliters) from one container to another.

2.1. Synthesis of quinoline derivatives

This study was carried out with methoxy substituted quinolines (**8–16, 19–20**) according to our previous papers [11,33–36]. In brief, the synthesis of methoxy quinolines and tetrahydroquinolines (**8–9**), were prepared by cupper induced substitution reactions of corresponding bromo tetrahydroquinoline and bromo quinoline derivatives [7,11,33–36]. The brominated methoxy quinoline derivatives (**6–11**) via treatment of molecular bromine (**8–16, 19–20**) were synthesized according to our reported procedures [7,11,34–36]. Furthermore, the synthesis of novel 5-nitro-8-methoxyquinoline (**20**) and 5-nitro-6, 8-dibromoquinoline (**17**) via nitration of 8-methoxyquinoline (**18**) and 6,8-dibromoquinoline (**5**), respectively were reported in our recent works [11,35]. The isolated compounds **8–17** and **19–20** were fully characterized by melting point, HRMS analysis, infrared, ^{1}H, ^{13}C, HMBC and HETCOR spectroscopy in these papers [7,34–36]. All tested compounds were purified by column chromatography and reduced atmospheric pressure as 99.9 %. The purity of tested compounds was monitored with ^{1}H NMR spectroscopy.

2.2. Synthesis of 5-nitro-8-methoxyquinoline (20)

8-Methoxyquinoline (**16**) (0.50 g, 3.14 mmol) was dissolved in 5 mL of sulfuric acid and cooled at −5 °C using a salt-ice bath. A mixture of sulfuric acid (4 mL) and nitric acid (4 mL) was prepared and cooled at −5 °C. The resulting solution was then cooled at 0 °C on a salt-ice bath for a few minutes. While stirring the solution of 8-methoxyquinoline (**16**) with a magnetic stirrer, the sulfuric acid/nitric acid mixture was added dropwise using a Pasteur pipette over the course of 1 h, ensuring that the solution temperature did not exceed 0 °C. After 2 h, the reaction was complete, and the reaction mixture was poured onto crushed ice (30 g) in a beaker. Once the ice had melted, the mixture was extracted with dichloromethane (5 × 20 mL). The organic phase was neutralized with a 10 % aqueous sodium bicarbonate ($NaHCO_3$) solution and dried over sodium sulfate (Na_2SO_4). The solvent was then removed under vacuum, and the resulting residue was filtered over silica. The ^{1}H NMR analysis indicated the formation of two products. The mixture of products was applied to a short silica gel chromatography column, eluting with hexane (100 mL). The first eluent (100–800 mL) yielded 5,7-dinitro-8-methoxyquinoline (222 mg, isolated yield 87 %) in a mixture of ethyl acetate (AcOEt) and hexane (1:4). The solvent polarity was then increased to a 1:2 (AcOEt/hexane) ratio, resulting in the separation of 5-nitro-8-methoxyquinoline (**20**) in pure form (58 mg, 9 %).

*5-nitro-8-methoxyquinoline (**20**)*: White neddlecrystal, yield 9 %, m. p.: 141–144 °C. **^{1}H-NMR** (400 MHz, $CDCl_3$, δ, ppm): δ_H 9.25 (d, J_{43} = 8.8 Hz, 1H, H_4), 9.05 (dd, J_{24} = 1.6 Hz, J_{23} = 4.0 Hz, 1H, H_2), 8.56 (d, J_{67} = 8.8 Hz, 1H, H_6), 7.72 (dd, J_{32} = 4.0 Hz, J_{34} = 8.8 Hz, 1H, H_3), 7.10 (d, J_{76} = 8.8 Hz, 1H, H_7), 4.23 (s, 3H, OMe). **^{13}C-NMR** (100 MHz, $CDCl_3$ δ, ppm): δ_C 160.8, 150.2, 139.4, 137.6, 136.6, 127.6, 124.6, 123.0, 105.3, 56.9 (OMe). **FTIR** (ν_{max}, cm^{-1}): 3108, 3015, 2957, 1612, 1578, 1497, 1388, 1269, 1180, 957, 898, 762, 716, 603. Anal. calcd. for $C_{10}H_8N_2O_3$ (204.0535): C, 58.82 %; H, 3.95 %; N, 13.72 %. Found: C, 58.47 %; H, 3.79 %; N, 13.80 %.

2.3. Synthesis of 6,8-dibromo-5-nitroquinoline (17)

A solution of 6,8-dibromoquinoline (**5**) (1.00 g, 3.484 mmol) in 10 mL of sulfuric acid was cooled to −5 °C in a salt-ice bath and treated slowly with a solution of 50 % nitric acid in 20 mL of sulfuric acid at

−5 °C while stirring the 6,8-dibromoquinoline (**5**) solution. After 1 h in an ice bath, the yellow mixture was allowed to warm up to room temperature. The resulting red solution was poured onto crushed ice (50 g) in a beaker. After the ice melted, the mixture was extracted with CH_2Cl_2 (3 × 40 mL). The organic phase was neutralized with a 10 % aqueous $NaHCO_3$ solution and dried over Na_2SO_4. The solvent was removed under vacuum. Yellow needle-shaped crystals were obtained as the sole product **17** with a yield of 96 % (1.106 g). M. p. 160–162 °C. **^{1}H NMR** (400 MHz, $CDCl_3$): δ 9.17 (dd, $J_{23} = 4$ Hz, $J_{24} = 1.2$ Hz, 1H, H_2), 8.33 (s, 1H, H_7), 8.08 (dd, $J_{42} = 1.2$ Hz, $J_{43} = 4$ Hz, 1H, H_4), 7.69 (dd, $J_{32} = 4$ Hz, $J_{34} = 4$ Hz, 1H, H_3). **^{13}C NMR** (100 MHz, $CDCl_3$): δ 152.6, 147.3 (q), 143.9 (q), 135.7, 130.6, 128.8 (q), 124.6 (q), 121.9 (q), 112 (q). **FTIR** (cm^{-1}): 3083, 2958, 2862, 1583, 1536, 1519, 1471, 1371, 1340, 1290, 1199, 927, 873, 856, 806, 779. Anal. Calcd for $C_9H_4Br_2N_2O_2$ (331.95 g/mol): C, 32.56 %; H, 1.21 %; N, 8.44 %. Found C, 32.42 %; H, 1.25 %; N, 8.47 %.

2.4. Acetylcholinesterase method

The potential inhibitory effect of methoxyquinoline derivatives on the enzyme AChE was investigated using the acetylcholinesterase method [37] under *in vitro* conditions. Spectrophotometric measurements were used to calculate IC_{50} values and Lineweaver-Burk diagrams were used to determine K_i values. Tacrine was used as the standard in the study and results were compared. The enzyme inhibitory potential of the compounds for AChE was determined using the following method: Combine the enzyme solution, Tris-HCl, H_2O and inhibitor solutions in a 1 mL cuvette, adding the substrates (DTNB and acetylcholine iodate) last. The resulting mixture is then measured spectrophotometrically.

Our method is based on measuring the color intensity of the yellow 5-thio-2-nitrobenzoic acid compound at 412 nm. This color results from the interaction between thiocholine, a degradation product formed by the AChE enzyme catalyzing the hydrolysis of acetylcholine, and DTNB used in inhibition studies. Absorbances of the sample and blank cuvettes are measured at the beginning and after the 5th minute [37] to determine the degree of inhibition.

2.5. Esterase method

To evaluate the potential inhibitory effect of methoxyquinoline derivatives on hCA I and II enzymes, we used the esterase activity method for kinetic and inhibitory studies [38]. Spectrophotometric measurement was performed at 348 nm, and IC_{50} values were calculated using the obtained data. K_i values were determined from Lineweaver-Burk plots. The method is based on the fact that hCA exhibits esterase activity and that the enzyme hCA hydrolyzes *p*-nitrophenyl acetate, which is used as a substrate, to *p*-nitrophenol or *p*-nitrophenolate, which absorbs at 348 nm. The enzyme activity was determined using the following method: Combine the Tris-SO_4 (0,5 M) pH 7.4, H_2O and inhibitor solutions in a 1 mL quartz cuvette, adding the substrate (*p*-Nitrophenol acetate) last. The resulting mixture is then measured spectrophotometrically.

The amount of water was adjusted to compensate for the increase in enzyme volume, and the total volume was always brought to 1000 μL. Following the preparation of the reaction mixture, the absorbance at 348 nm at 25 °C was measured at the beginning and end of 3 min, and the difference was recorded.

2.6. Antimicrobial activity

In this study, to detection of MIC values of the compounds; 2 g-negative bacteria (*Escherichia coli* (ATCC 25922) and *Pseudomonas aeruginosa* (ATCC 27853)), 2 g-positive bacteria (*Staphylococcus aureus* (ATCC 29213) and Bacillus cereus (ATCC 11778)) and two yeast strain (Candida albicans (ATCC 10231) and *Candida tropicalis* (DSM 11953)) were used. The MIC values of the synthesized compounds were determined by microdilution techniques in Mueller-Hinton broth (Accumix®AM1072) for bacteria and Sabouraud Dextrose Broth (Himedia ME033) for yeast (CLSI, 2002, CLSI, 2012).

The compounds were dissolved in DMSO (10 mg/mL). 90 μL of media were added to the first row of the microliter plates and 50 μL of the remaining wells. The 11th wells were used as the reproductive controls and 100 μL broth was added. 50 μL of microorganism and 50 μL of broth was added to 12 th column for as reproductive control. 10 μL compounds was added in the first line of the microtiter plate and serial two-fold dilutions were prepared. The concentration of the compounds in the wells was ranging from 500 to 0.976 μg/mL. The bacteria and yeast suspensions (50 μL) were added to prepared samples. The final inoculum size was 5×10^5 CFU/mL in the bacteria wells and 0.5–2.5 × 10^3 CFU/mL in the Candida sp. wells (CLSI, 2002, CLSI, 2012). The microtiter plates were incubated at 37 °C and the MICs were recorded after 24 h of incubation. The MIC was defined as the lowest concentration of the compounds at which the microorganism tested did not demonstrate visible growth.

2.7. Geometry optimizations and dock studies

In the initial phase of our computational analysis, we conducted conformational searches and geometry optimizations for thirteen newly synthesized molecules. This was achieved using the semi-empirical PM6 method as described by Stewart [39,40]. The computations were performed using Spartan'16 V1.1.4 software, developed by Hehre et al. [41].

For the subsequent docking studies, we selected Carbonic Anhydrase (hCA I PDB ID: 5E2M), Carbonic Anhydrase II (hCA II PDB ID: 6KM3), and Acetylcholinesterase (AChE) (PDB ID: 2COP) enzymes as the target macro structures. The active site amino acids of these proteins were enclosed within a grid box measuring 40 × 40 × 40 $Å^3$. The grid box coordinates for the active regions of the respective protein structures are provided in Table 1 below.

All the docking experiments and visualizations were conducted using the following software tools: AutoDock 4.2 [42,43] and AutoDock Vina [44]. Visualization of the results was performed using BIOVIA Discovery Studio Visualizer, developed by Dassault Systèmes BIOVIA [45].

3. Results and discussion

3.1. Synthesis

In our previous studies, we synthesized a series of brominated quinoline derivatives (**3**–**7**) [7,33] (Scheme 1) and converted them into corresponding methoxide derivatives (**8**, **9**, **13**, **15**) by treatment with NaOMe, using procedures previously reported (Scheme 2) [7,34,35]. We then subjected the methoxy derivatives to further bromination to prepare the corresponding bromomethoxy quinoline analogues **(10**–**12**, **14**, **16**, and **19)** using procedures described in our previous work (Scheme 2) [34,36]. Additionally, we investigated the reaction of 6,8-dibromoquinoline (**5**) and 8-methoxyquinoline (**18**) with an HNO_3/H_2SO_4 mixture. The nitration of 6,8-dibromoquinoline (**5**) resulted in the formation of novel 5-nitro-6,8-dibromoquinoline (**17**) in high yield (96 %) as a sole while treatment of 8-methoxyquinoline (**18**) with an HNO_3/H_2SO_4 mixture furnished a mixture of novel 5-nitro-8-methoxyquinoline (**20**) and 5,7-dinitro-8-methoxyquinoline [11] (Scheme 2) [36]. The products, 5-nitro-8-methoxyquinoline (**20**) and 5,

Table 1
XYZ coordinates for the active sites of the related proteins.

PDB ID	X	Y	Z
2COP	28.701	15.686	12.434
5E2M	5.212	73.538	57.12
6KM3	19.215	−9.422	16.113

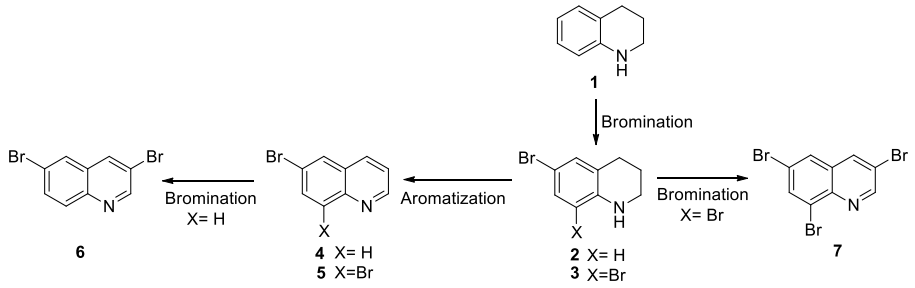

Scheme 1. Synthesis of brominated tetrahyroquinoline and quinoline derivatives as starting compounds **(2–7).**

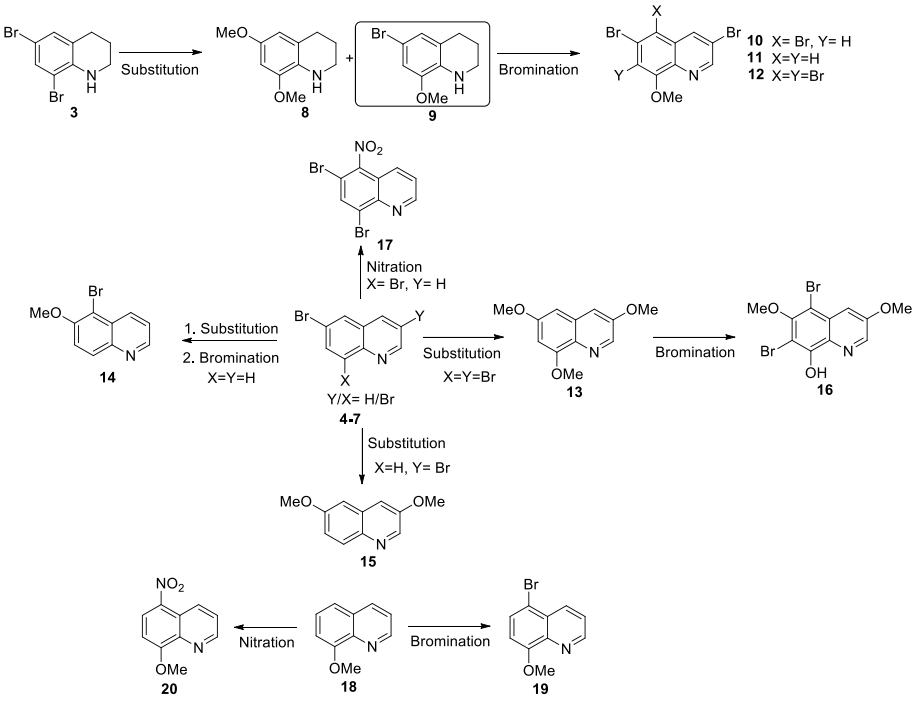

Scheme 2. Synthesis of methoxy quinolines (**2**, **8**, **13** and **15**) and their brominated and nitrated analogues (**10–12**, **14**, **16–17** and **19–20**).

7-dinitro-8-methoxyquinoline, were isolated by column chromatography in yields of 9 % and 87 %, respectively.

The structures of nitrate-containing compounds **17** and **20** were determined using various analytical techniques, including ^{1}H NMR, ^{13}C NMR, FT-IR and elemental analysis. In the ^{1}H NMR spectra of compound **17**, the disappearance of two doublets with meta coupling observed in starting material **5** and the appearance of a new singlet δ_H 8.33 ppm [7] in the aromatic region indicated the binding of nitro group to quinoline ring at C-5 position. Additionally, the chemical shift values of the other aromatic signals were observed to shift downfield due to the presence of the NO_2 group. In the NMR spectrum of the starting material **5** [7], the characteristic H-2 signal at δ_H 9.04 (dd, $^{3}J = 4.2$ Hz, $^{4}J = 1.6$ Hz) shifted to δ_H 9.17 (dd, $^{3}J = 4$ Hz, $^{4}J = 1.2$ Hz) in ^{1}H NMR spectra of compound **17**. In the FT-IR spectra of 6,8-dibromo-5-nitroquinoline (**17**), the strong C–N stretching bands were observed at 1290 and 1199 cm^{-1}. The characteristic vibrations belong to the aromatic C–H stretchings were detected at ca. 3083-2862 cm^{-1}. Furthermore, in the FT-IR spectra of **17**, a characteristic N═O stretching signals were observed at 1583 and 1340 cm^{-1}.

In the ^{1}H NMR spectrum of compound **20**, the characteristic doublet of doublet for H-2 of the quinoline scaffold was observed at 9.05 ppm ($^{4}J = 1.6$ Hz, $^{3}J = 4.0$ Hz). The signals for the aromatic protons H-3 and H-4 (δ_H 7.72, $^{3}J = 4.0$ Hz and $^{3}J = 8.8$ Hz; 9.25, $^{3}J = 8.8$ Hz, respectively) were found to be shifted further downfield compared to signals of the starting material. The proton of the benzene ring of **20** appeared as doublets in the downfield region at δ_H 8.56 and 7.10 ($^{3}J = 8.8$ Hz), indicating the presence of bromine at C-6 and C-7, respectively. It was observed that the signals of H-5 disappeared after nitration when compared to the signal pattern of the starting material **18**[11], providing evidence for nitration occurring at both the C-5 positions. In the FT-IR spectra of 8-methoxy-5-nitroquinoline (**20**), the C–N stretching bands were detected at 1269 and 1180 cm^{-1}. The characteristic vibrations belong to the aromatic C–H stretchings were observed at ca. 3108-2957 cm^{-1}. Furthermore, in the FT-IR spectra of **20**, a characteristic N═O stretching signals were observed at 1578 and 1388 cm^{-1}.

3.2. Enzyme inhibition studies

Based on the test results, it appears that the compounds were tested for their inhibitory activity against two isoforms of hCA. The IC_{50} values represent the concentration of the compound required to inhibit the enzyme activity by 50 %, while the K_i values represent the binding affinity of the compound for the enzyme.

It appears that most of the compounds showed strong inhibition of both hCA I and hCA II, with IC_{50} values ranging between 0.13 and 21.38 μM, compared to the control compound AZA (Acetazolamide) (IC_{50} = 18.11 μM for hCA I and IC_{50} = 20.65 μM for hCA II). However, compounds **10** and **13** exhibited weak inhibitory potential against both

enzymes, with IC_{50} values ranging from 36.52 to 99.02 μM. The compounds also showed relatively good binding affinity for both enzymes, as demonstrated by their K_i values.

The test results indicate that compounds **12**, **17**, and **9** are effective inhibitors of hCA I enzyme, with IC_{50} values of 1.54, 4.22, and 4.31 μM respectively. However, compounds **10** and **13** showed weak inhibitory potential against hCA I with IC_{50} values of 48.85 and 36.52 μM, respectively which is less effective than the control compound AZA with an IC_{50} value of 18.11 μM. In contrast, compounds **17**, **16**, **12**, and **9** demonstrated significant inhibition of hCA II, with IC_{50} values of 0.13, 0.72, 1.12, and 4.26 μM respectively. However, compounds **10** and **13** exhibited weak inhibition of hCA II, with IC_{50} values of 45.85 and 99.02 μM respectively. Compound **14** exhibited inhibition of hCA II (IC_{50} = 18.54 μM), but its inhibition of hCA I (IC_{50} = 21.38 μM) was weaker (Table 2).

Based on the test results, it appears that the compounds were indeed tested for their inhibitory activity against the enzyme AChE. Among the tested compounds, **8** and **13** exhibited the strongest inhibition of AChE with IC_{50} values of 3.15 and 4.96 μM respectively, indicating their potential as AChE inhibitors. Meanwhile, compounds **11** and **15** showed moderate inhibition of AChE, with IC_{50} values of 98.57 and 82.75 μM respectively. However, compound **9** exhibited very weak inhibition of AChE, with an IC_{50} value of 1407.03 μM, suggesting that it is unlikely to be effective as an AChE inhibitor (Table 3).

3.3. Antimicrobial evaluation of the compounds

The antimicrobial activities of **8**–**11**, **13**–**15** and **19**–**20** compounds against some pathogenic bacteria and yeasts causing diseases in the human body were determined using the Minimum Inhibition Concentration (MIC) method. When the MIC values of compounds displayed on Gram (+) bacteria were examined, it found that only two compounds, 3,6,8-trimethoxylquinoline (**13**) and 3,6-dimethoxylquinoline (**15**) derivatives have moderately inhibited the proliferation of all of Gram (+) bacteria (MIC values ranging from 125 to 250 μg/mL), however, compounds **10** and **20** selectively displayed good inhibition against *B. cereus* (ATCC11778) (MIC values, 62.5 and 125 μg/mL, respectively) (Table 4).

Table 2
IC_{50} and K_i values of tested compounds (**8**–**20**) against hCA I and II.

Compounds	IC_{50} (μM)				K_i (μM)	
	hCA I	r^2	hCA II	r^2	hCA I	hCA II
8	**5.42**	0.9958	**6.93**	0.9969	**30.83 ± 1.74**	**4.22 ± 4.16**
9	**4.31**	0.9643	**4.26**	0.9951	**31.97 ± 1.15**	**113.38 ± 7.10**
10	48.85	0.9983	45.85	0.9475	**55.53 ± 29.12**	**29.76 ± 24.58**
11	**6.19**	0.9476	**13.65**	0.9308	**17.22 ± 2.52**	**75.27 ± 33.63**
12	**1.54**	0.9798	**1.12**	0.9321	**179.343 ± 37.96**	**59.22 ± 22.75**
13	36.52	0.9216	99.02	0.9797	322.70 ± 153.50	654.24 ± 41.42
14	21.38	0.9623	18.54	0.8465	**7.78 ± 2.7**	**1.24 ± 0.98**
15	**9.11**	0.8557	**5.86**	0.9521	**73.56 ± 47.46**	**69.32 ± 5.14**
16	**5.77**	0.9516	**0.72**	0.9855	**30.20 ± 9.68**	**73.49 ± 19.48**
17	**4.22**	0.9759	**0.13**	0.9394	**155.32 ± 14.94**	**12.26 ± 7.02**
19	**8.67**	0.9984	**9.48**	0.8477	**11.99 ± 9.59**	**72.41 ± 7.37**
20	**5.99**	0.8475	**11.50**	0.7597	**96.43 ± 65.59**	880.61 ± 101.83
AZA	**18.11**	**0.9387**	**20.65**	**0.9756**	**271.15 ± 74.62**	**113.07 ± 20.98**

Table 3
IC_{50} and K_i values of tested compounds (**8**, **9**, **11**, **13**, **15**) against AChE.

Compounds	IC_{50} (μM)	
	AChE	r^2
8	**3.15**	0.9968
9	1407.03	0.9518
11	98.57	0.8929
13	**4.96**	0.9418
15	82.75	0.9765
Tacrine	53.31	0.9698

On the other hand, only compounds 13 and 15 were moderately effective against *E. coli* (ATCC25922) in MIC value of 250 μg/mL. According to the MIC values of recently synthesized compounds against fungus, most of the compounds showed effective inhibition against *C. Albicans* ATCC10231 and *C. Tropicalis* DSM11953 (125–250 μg/mL) fungi, while good inhibition of 3,6,8-trimethoxylquinoline (**13**) was observed against only C. albicans ATCC10231 (62.50 μg/mL) (Table 4).

As a result, it is clear that compounds **13** and **15** have promising antimicrobial activity for future studies. Especially, quinolines **15** and **13** bearing two methoxy groups at C-3 and C-6 were more active against microorganisms than brominated methoxy tetrahydroquinoline and quinoline derivatives (**8**–**11**, **14, 19**–**20**).

3.4. Molecular docking studies

In the computational aspect of this study, we conducted docking experiments involving thirteen molecules with proteins encoded by the PDB IDs 2COP, 5E2M, and 6KM3. Subsequently, we analyzed the results obtained from these docking studies, focusing on binding energy values (BE) measured in kcal/mol. We also identified the pivotal amino acids located within the active regions of the enzymes, elucidating the types of interactions and their respective distances.

The calculated binding energy (BE) values, along with the interaction types and distances, have been meticulously documented in Tables 5 and 1S. These interactions play a critical role in the identification of essential amino acids within the active sites of the examined proteins. Consequently, we present a comprehensive list of the interacting amino acids, as well as the associated interaction types and distances, between the proteins 2COP, 5E2M, 6KM3, and the respective molecules in Table 1S.

Upon closer examination of Table 1S, we can observe the binding affinity values calculated for the protein structures encoded by PDB IDs 2COP, 5E2M, and 6KM3. Specifically, for the 2COP structure, the binding affinity ranges from −7.9 kcal/mol to −6.7 kcal/mol, while for the 5E2M structure, it varies from −5.3 kcal/mol to −6.9 kcal/mol. In the case of the 6KM3 structure, the binding affinity falls within the range of −6.2 kcal/mol to −7.2 kcal/mol. Notably, the most stable binding interactions are observed with the 2COP structure, whereas the weakest interactions are found with the 5E2M structure.

Upon further examination of the binding energies of the compounds, it becomes evident that the most favorable interactions with the 2COP structure are exhibited by compounds **16**, **17**, **12**, and **10** with binding energy values of −7.9 kcal/mol, −7.7 kcal/mol, −7.4 kcal/mol, and −7.4 kcal/mol, respectively. Additionally, with the 5E2M structure, compounds **16**, **17**, and **9** demonstrate favorable interactions, with binding energy values ranging from −5.8 kcal/mol to −6.9 kcal/mol. Conversely, the 6KM3 structure shows strong interactions with compounds **20** (−7.2 kcal/mol), **18** (−7.0 kcal/mol), **9** (−6.9 kcal/mol), and **16** (−6.9 kcal/mol).

These findings provide valuable insights into the binding affinities and preferences of the studied compounds with respect to the 2COP, 5E2M, and 6KM3 protein structures.

The most influential amino acids within the active region of the 2COP PDB ID-encoded structure, based on their interactions and

Table 4
Minimum-inhibitory concentrations (MIC, μg/mL) of the compounds (**8–11, 13–15, 19–20**) against microorganisms.

Comp. #	Gram (+)		Gram (−)		Yeast	
	S. aureus ATCC29213	*B. cereus* ATCC11778	*E. coli* ATCC25922	*P. aeruginosa* ATCC27853	*C. albicans* ATCC10231	*C. tropicalis* DSM11953
8	>500	>500	>500	>500	**250**	>500
9	>500	>500	>500	>500	**125**	**125**
10	>500	**62.5**	>500	>500	**250**	>500
11	>500	>500	>500	>500	>500	>500
13	**250**	**125**	**250**	>500	**62.5**	**125**
14	500	250	>500	>500	**125**	**125**
15	**250**	**125**	**250**	>500	**125**	**125**
19	500	500	>500	>500	**125**	**125**
20	500	**250**	500	>500	**125**	**125**
SCF	62.50	7.81	15.62	250	15.62	15.62

SCF: Sulbactam (30 μg) + cefoperazone (75 μg), as a positive control.

Table 5
Calculated Binding Energy (BE) values (kcal.mol^{-1}) of the molecules (**8–20**) with interacted amino acids.

Compounds	Calculated Binding Energy (BE) values (kcal.mol^{-1})		
	2COP	5E2M	6KM3
8	−6.9	−5.7	−6.8
9	−6.9	−5.8	−6.9
10	−7.4	−5.4	−6.5
11	−7.1	−5.4	−6.3
12	−7.4	−5.4	−5.9
13	−6.9	−5.5	−6.7
14	−6.9	−5.3	−6.2
15	−6.7	−5.7	−6.7
16	−7.9	−6.9	−6.9
17	−7.7	−6.0	−6.7
18	−6.7	−5.7	−7.0
19	−6.8	−5.3	−6.4
20	−6.9	−5.7	−7.2

distances with ligands, include TRP86, SER125, LEU130, Y337, and HIS447 amino acids. Notably, TRP86 in the active region engages in π-σ bond interactions with all the studied ligands within the range of 3.67–4.87 Å. Additionally, amino acid SER125 consistently forms hydrogen bond interactions in all interactions.

In contrast, when examining the binding interactions between ligands and the 5E2M PDB ID-encoded structure, another protein structure used in the docking studies, it becomes evident that longer and weaker interactions occur, resulting in lower binding energies. Among all the ligands studied, it has been observed that hydrogen bonds, one of the strongest intermolecular interaction types, are exclusively formed between amino acid THR99 and LEU20.

Lastly, in the interactions derived from the docking studies conducted for the 6KM3 PDB ID-encoded structure, amino acids HIS64, HIS94, VAL121, PHE131, LEU198, THR199, and THR200 in the active site structure exhibit the most significant bonding with the ligands, and these interactions occur at close range.

Remarkably, compound **16** emerges as the best-interacted ligand, displaying the strongest interactions with all three studied crystal structures, as detailed in Table 6.

3.5. Discussion

The study explored the inhibitory effects of substituents on the quinoline and tetrahydroquinoline cycle. Findings revealed that the introduction of methoxy groups at positions C-6 and C-8 in compounds **8** and **9** led to heightened inhibition against hCAI and hCA II isoenzymes in comparison to the initial compound **3** [11].

The presence of methoxy groups at the C-6 and C-8 positions in compound **8** displayed substantial inhibition against the AChE enzyme. However, the introduction of a bromine atom at the C-6 position in compound **9** led to a notable decrease in inhibition. Similarly, compound **13**, with methoxy groups at both the C-6 and C-8 positions, significantly inhibited the AChE enzyme, while compound **15**, bearing a methoxy group only at the C-6 position, exhibited slight inhibition. These observations imply that the presence of methoxy groups at the C-8 positions of the benzenoid ring in tetrahydroquinoline **9** and at both C-6 and C-8 positions within the quinoline structure of compound **13** plays a crucial role in inhibiting the AChE enzyme.

Additionally, it plays a crucial role in enhancing the methoxy group's activity at both the C6 and C-8 positions within the benzene moiety of the tetrahydroquinoline ring, thereby affecting the inhibition of cytosolic carbonic anhydrase and choline energetic enzymes. This is supported by the fact that substituting the methoxy group with a bromine atom at the C-6 position of compound **9** significantly diminished the inhibition of the AChE enzyme. Interestingly, introducing a bromine atom at the C-6 position of compound **9** did not adversely affect the inhibition of hCA I and hCA II enzymes. There was no noteworthy impact observed on the inhibition of carbonic anhydrase enzymes upon bromination of the tetrahydric prenoid ring (**11**). However, the formation of tribromide (**10**) through advanced bromination of the ring containing methoxy groups notably reduced enzyme inhibition. Conversely, the aromatization of compound **9** via bromination at the C-3 position significantly increased the inhibition of the AChE enzyme. These findings imply the significance of aromatization of the quinoline ring and bromination at the C-3 position in influencing both hCA enzymes and AChE enzymes.

We conducted a study on the inhibitory effects of aromatic quinoline compounds that are trisubstituted at the C-3, C-6, and C-8 positions against hCA I, hCA II and AChE enzymes. Our findings revealed that 3,6,8-tribromoquinoline (**7**) had significant inhibitory properties against all three enzymes [11]. However, substitution of the three bromine atoms with a methoxy group in compound **13** considerably decreased inhibition against cytosolic hCA I and hCA II enzymes compared to the control compound. Despite this, compound **13** exhibited high inhibitory activity against the AChE enzyme. Additionally, compound **15**, which lacked a methoxy group at the C-8 position, demonstrated good inhibition against hCA enzymes, suggesting that the C-8 position is crucial for inhibitory activity against AChE enzyme. Furthermore, we found that 5,7-dibromo-3,6-dimethoxy-8-hydroxyquinoline (**16**), showed more effective inhibitory properties against hCA enzymes than its starting material (**13**). This could be attributed to the conversion of the methoxy group at the C-8 position to a hydroxy group.

The bromination and nitration of 8-methoxyquinoline produces compounds that exhibit excellent enzyme inhibition. In our previous study, we observed that 5,7-dibromo-8-methoxyquinoline and 5,7-dinitro-8-methoxyquinoline had high inhibitory activity against enzymes [11]. Similarly, 5-bromo-8-methoxyquinoline (**19**) and 5-nitro-8-methoxyquinoline (**20**) displayed significant inhibitory activities against cytosolic carbonic anhydrase enzymes. This suggests that the nitro and bromine groups at the C-5 position and the methoxy group

Table 6
Depicted 2D and 3D interaction maps between compound **16** and studied crystal structures by docking simulations.

PDB ID	2D interaction maps	3D polarity maps
2COP	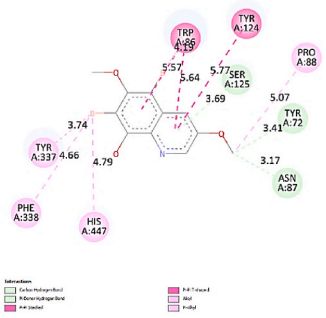	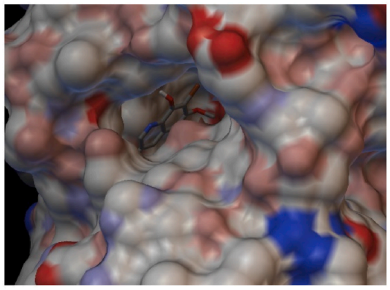
5E2M	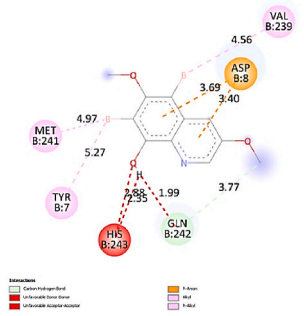	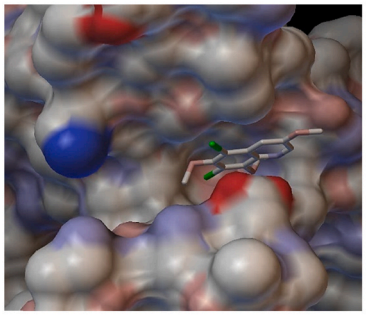
6KM3	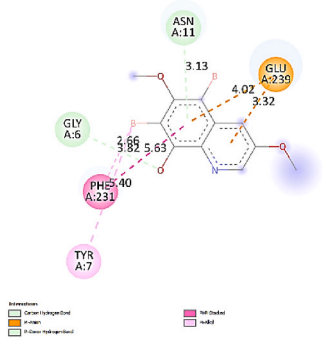	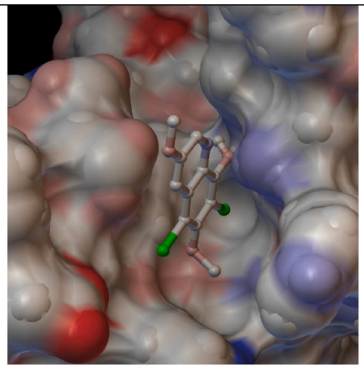

at the C-8 position are crucial for activity. Moreover, the significant inhibition exhibited by 6,8-dibromo-5-nitroquinoline highlights the importance of the nitro group at the C-5 position. These results provide further evidence that the activity of these compounds is influenced by the position and type of substituents.

The *in-silico* study has successfully validated the experimental results. Functionalized methoxy quinoline derivatives (**8**–**20**) exhibited strong binding affinities ranging from 5.9 to 7.2 kcal/mol. These compounds, especially containing OH and NH groups in their structure of **8**, **9** and **17**, engage in hydrogen bond interactions with specific residues of the hCA II protein, including TRY7, GLY8, HIS64, HIS94, HIS119, HIS96, THR119, and THR200. Furthermore, these same compounds **8**, **9** and **17** demonstrated high binding potential towards residues of the hCA I protein, forming polar interactions and hydrogen bonds with ASP108, HIS64, HIS94, HIS96, HIS119, VAL121, THR200, LEU198, and GLU239. Notably, compounds **16** and **17** displayed remarkable binding capabilities with the selected proteins (2COP, 5E2M, 6KM3), suggesting their potential as strong binders in these interactions. This underscores their promising role in future research and applications.

4. Conclusion

The study explored the effects of synthesizing brominated quinoline derivatives and their transformations on enzyme inhibition and antimicrobial activity. Methoxy derivatives, especially compounds **8** and **13,** showed enhanced enzyme inhibition, particularly against carbonic anhydrase (hCA) and acetylcholinesterase (AChE) enzymes, with specific positions and substitutions playing crucial roles. By altering methoxy groups and introducing bromine or nitro substitutions at specific positions in the quinoline and tetrahydroquinoline rings, significant variations in enzyme inhibition were observed. Aromatization and bromination at certain sites notably influenced enzyme activity, highlighting the importance of these modifications. Compounds with unique substitutions exhibited varying degrees of inhibition against enzymes and displayed promising antimicrobial effects against select pathogens, notably compounds **13** and **15**. Molecular docking studies validated experimental findings, revealing compounds **8**–**20** as potent binders to target enzymes, emphasizing their potential for further investigations. This comprehensive study illuminates the intricate relationship between molecular structure and biological activity in brominated quinoline

derivatives, offering insights for potential drug development and therapeutic approaches.

CRediT authorship contribution statement

Bilge Çiftci: Data curation, Funding acquisition. **Salih Ökten:** Conceptualization, Formal analysis, Investigation, Methodology, Supervision, Writing – original draft, Writing – review & editing. **Ümit Muhammet Koçyiğit:** Conceptualization, Supervision. **Vildan Enisoğlu Atalay:** Data curation, Methodology, Writing – original draft. **Mehmet Ataş:** Data curation. **Osman Çakmak:** Supervision.

Declaration of competing interest

All authors declare that they have no conflict of interests.

Data availability

No data was used for the research described in the article.

Acknowledgement

This study was supported by project number "1919B012107879″ under the TUBITAK-Scientist Support Programs Presidency (BIDEB) 2209-A College Students Research Projects Support Program.

Appendix A. Supplementary data

Supplementary data to this article can be found online at https://doi.org/10.1016/j.ejmcr.2023.100127.

References

[1] X.M. Chu, C. Wang, W. Liu, L.L. Liang, K.K. Gong, C.Y. Zhao, K.L. Sun, Eur. J. Med. Chem. 161 (2019) 101.
[2] L. Dobbin, J. Chem. Educ. (1934) 596.
[3] M.E. Wall, M.C. Wani, C.A. Cook, K.H. Palmer, A.A. McPhail, G.A. Sim, J. Am. Chem. Soc. 88 (1966) 3888.
[4] V. Gasparotto, I. Castagliuolo, G. Chiarelotto, V. Pezzi, D. Montanaro, P. Brun, G. Palù, G. Viola, M.G. Ferlin, J. Med. Chem. 49 (2006) 1910.
[5] D.R. Boyd, N.D. Sharma, P.L. Loke, J.F. Malone, W.C. McRoberts, J.T.G. Hamilton, Org. Biomol. Chem. 5 (2007) 2983.
[6] A. Marella, O.P. Tanwar, R. Saha, M.R. Ali, S. Srivastava, M. Akhter, M. Shaquiquzzaman, M.M. Alam, Saudi Pharmaceut. J. 21 (2013) 1.
[7] S. Ökten, O. Çakmak, R. Erenler, Ö.Y. Şahin, Ş. Tekin, Turk. J. Chem. 37 (2013) 896.
[8] B. Meunier, Acc. Chem. Res. 41 (2008) 69.
[9] M.S. Shaveta, P. Singh, Eur. J. Med. Chem. 124 (2016) 500.
[10] H. Wang, H. Zhang, ACS Chem. Neurosci. 10 (2019) 852.
[11] S. Ökten, A. Aydın, Ü.M. Koçyiğit, O. Çakmak, S. Erkan, C.A. Andac, P. Taslimi, İ. Gülçin, Arch. Pharm. 353 (2020) e2000086.
[12] S. Kamaal, A. Ali, M. Afzal, M. Muslim, A. Alarifi, M. Ahmad, Chem. Pap. 76 (2022) 5177–5186.
[13] A. Ali, N. Sepay, M. Afzal, N. Sepay, A. Alarifi, M. Shahid, M. Ahmad, Bioorg. Chem. 110 (2021) 104772.
[14] A. Ali, S. Banerjee, S. Kamaal, M. Usman, N. Das, M. Afzal, A. Abdullah, N. Sepay, P. Roy, M. Ahmad, RSC Adv. 11 (2021) 14362–14373.
[15] M. Hagrs, A.H. Bayoumi, K.M. El-Gamal, A.S. Mayhoub, H.S. Abulkhair, Beni-Suef University J. Basic Appl. Sci. 4 (2015) 338.
[16] P. Hochegger, J. Dolensky, W. Seebacher, R. Saf, M. Kaiser, P. Mäser, R. Weis, Molecules 26 (2021) 5530.
[17] S.M. Aboutorabzadeh, F. Mosafa, F. Hadizadeh, R. Ghodsi, J. Iranian, Basic Med. Sci. 21 (2018) 9.
[18] H. Pajouhesh, G.R. Lenz, NeuroRx 2 (2005) 541.
[19] C. Roney, P. Kulkarni, V. Arora, P. Antich, F. Bonte, A. Wu, N.N. Mallikarjuana, S. Manohar, H.F. Liang, A.R. Kulkarni, H.W. Sung, M. Sairam, T.M. Aminabhavi, J. Contr. Release 108 (2005) 193.
[20] J. Fiorito, F. Saeed, H. Zhang, A. Staniszewski, Y. Feng, Y.I. Francis, S. Rao, D. M. Thakkar, S.X. Deng, D.W. Landry, O. Arancio, Eur. J. Med. Chem. 60 (2013) 285.
[21] C. Espinosa-Jovel, R. Toledano, Á. Aledo-Serrano, I. García-Morales, A. Gil-Nagel, Seizure 56 (2018) 67.
[22] R.S. Fisher, W. Van Emde Boas, W. Blume, C. Elger, P. Genton, P. Lee, J.J. Engel, Epilepsia 46 (2005) 470.
[23] C.T. Supuran, Nat. Rev. Drug Discov. 7 (2008) 168.
[24] A. Thiry, J.M. Dogné, C.T. Supuran, B. Masereel, Curr. Pharmaceut. Des. 14 (2008) 661.
[25] N.R. Wulf, K.A. Matuszewski, Am. J. Health Syst. Pharm. 70 (2013) 1483.
[26] M. Bortolami, F. Pandolfi, D. De Vita, C. Carafa, A. Messore, R. Di Santo, M. Feroci, R. Costi, I. Chiarotto, D. Bagetta, S. Alcaro, M. Colone, A. Stringaro, L. Scipione, Eur. J. Med. Chem. 198 (2020) 112350.
[27] E. Bagyinszky, V.V. Giau, Y.C. Youn, S.S.A. An, S. Kim, Neuropsychiatric Dis. Treat. 14 (2018) 2067.
[28] A.K. Thakur, P. Kamboj, K. Goswami, J. Anal. Pharm. Res. 7 (2018) 226.
[29] O. Çakmak, S. Ökten, D. Alimli, A. Saddiqa, C.C. Ersanlı, ARKIVOC (Gainesville, FL, U. S.) 2018 (2018) 362.
[30] O. Çakmak, S. Ökten, D. Alimli, C.C. Ersanlı, Ü.M. Koçyiğit, P. Taslimi, J. Mol. Struct. 1220 (2020) 128666.
[31] R. Patil, J.P. Chavan, A. Shivnath Beldar, Turk. J. Chem. 45 (2021) 1299.
[32] M. Ekiz, A. Tutar, S. Ökten, B. Bütün, Ü.M. Koçyiğit, P. Taslimi, G. Topçu, Arch. Pharm. 351 (2018) e1800167.
[33] S. Ökten, D. Eyigün, O. Çakmak, Sigma J. Eng. Nat. Sci. 33 (2015) 8.
[34] O. Çakmak, S. Ökten, Tetrahedron 73 (2017) 5389.
[35] S. Ökten, Z. Demircioğlu, C.C. Ersanli, O. Çakmak, Mol. Cryst. Liq. Cryst. 714 (2021) 37.
[36] O. Çakmak, S. Ökten, T. K. Köprülü, Ş. Tekin, Highly brominated quinolines: synthesis, chracterization and investigation of biological activities as cancer drug candidates, J. Biomol. Struc. Dyn., submitted for publication.
[37] G.L. Ellmann, K.D. Courtney, V.J. Andres, R.M. Feather-Stone, Biochem. Pharmacol. 7 (1961) 88.
[38] J.A. Verpoorte, S. Mehta, J.T. Edsall, J. Biol. Chem. 242 (1967) 4221.
[39] J.J.P. Stewart, J. Mol. Model. 14 (2008) 499.
[40] J.J.P. Stewart, J. Mol. Model. 15 (2009) 765.
[41] W.J. Hehre, H.F. Schaefer, J. Kong, A.I. Krylov, P.M.W. Gill, M. Head-Gordon, Phys. Chem. Chem. Phys. 8 (2006) 3172.
[42] S. Cosconati, S. Forli, A.L. Perryman, R. Harris, D.S. Goodsell, A.J. Olson, Expet Opin. Drug Discov. 5 (2010) 597.
[43] S. Forli, A.J. Olson, J. Med. Chem. 55 (2012) 623.
[44] O. Trott, A.J. Olson, J. Comput. Chem. 31 (2010) 455.
[45] Dassault Syst`emes BIOVIA, Discovery Studio Modeling Environment, Dassault Syst`emes, San Diego, 2016. Release 2017.